Journal of Statistical Physics, Vol. 93, Nos. 3/4, 1998

Physical Approaches to the Study of DNA

T. R. Strick,[1] J.-F. Allemand,[1] V. Croquette,[1] and D. Bensimon[1, 2]

Received February 17, 1998

New micromanipulation techniques now enable physicists and biologists to study the behavior of single biomolecules such as DNA. In particular, it is possible to measure the elastic response of individual DNA molecules to changes in the double helix's supercoiling. The force versus extension diagram for torsionally relaxed DNA is continuous and allows one to evaluate the persistence length of the polymer. When the molecule is supercoiled, however, stretching leads to the buildup of torsional stress in the double helix's axis. When the twist energy thus generated increases beyond a critical value, the molecule is locally destabilized and changes conformation. This structural transition occurs at stretching forces which can be exerted *in vivo* by molecular motors and at degrees of supercoiling found in the cell, and may have implications for DNA structure and function within the nucleus.

KEY WORDS: DNA micromanipulation; DNA supercoiling; DNA structural transitions; Brownian motion analysis.

I. INTRODUCTION

A. Primary Structure of DNA

The double-helical structure of deoxyribonucleic acid (DNA) is based on the right-handed winding of two constituent strands one around the other. The two strands interact via the formation of hydrogen bonds which stabilize the double helix. In contrast, the individual strand is constituted entirely of covalent bonds. Each strand is a polymer based on a three-subunit monomer, Fig. 1(A). The monomer, known as a nucleotide, consists

[1] Laboratoire de Physique Statistique de l'ENS, CNRS URA 1306, Associé aux Universités Paris VI et VII, 75231 Paris Cedex 05, France; e-mail: strick@clipper.ens.fr, allemand@physique.ens.fr, vincent@physique.ens.fr.

[2] Department of Complex Systems, Weizmann Institute, Rehovoth, Israel: e-mail: david@physique.ens.fr.

0022-4715/98/1100-0647$15.00/0

of a deoxyribose sugar molecule bearing on one side a purine or pyrimidine group (the "base") and on the other a phosphate group. The purines adenine (A) and guanine (G) and the pyrimidines cytosine (C) and thymine (T) differentiate the nucleotides and constitute the genetic code (an additional purine uracil (U) is found in ribonucleic acid (RNA)). A nucleotide is linked to its neighbors via phospho-diester bonds between

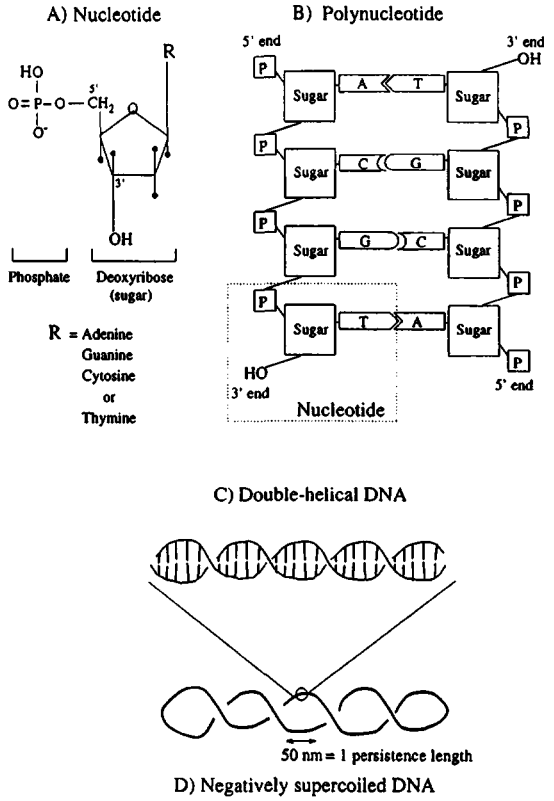

Fig. 1. The DNA molecule. (A) The monomer, or nucleotide, consists of a deoxyribose sugar bearing a phosphate group at the 5' carbon and a purine or pyrimidine base at the 1' carbon. The four nucleotides are differentiated by the purine (adenine or guanine) or pyrimidine (cytosine or thymine) group presented. (B) A flattened drawing of the DNA molecule. Each nucleotide is bound via phosphodiester bonds to its neighbors: the nucleotide's 5' phosphate binds to its neighbor's 3' OH group. The sequence of nucleotides constitutes the molecule's primary structure. (C) A sketch of the double helix showing the base-pairs at the molecule's core and the outer phosphate-sugar backbone; this represents the molecule's secondary structure. (D) The tertiary structure of a negatively supercoiled DNA as observed naturally in plasmids (circular DNA) presents interwound structures known as plectonemes.

the phosphate group and the ribose sugar, giving the strand an alternating sugar-phosphate backbone, see Fig. 1(B). Adenine and thymine nucleotides on opposite strands can interact via the formation of two hydrogen bonds between the purine and pyrimidine to form "base-pairs," while the guanine and cytosine nucleotides interact via three hydrogen bonds. The two strands of a regular DNA molecule normally carry complementary sequences, maximizing the number of hydrogen bonds holding them together. The canonical form of DNA *in vivo* is the so-called B-form, which has a rise per base-pair of about 3.4 Å and forms a helical turn roughly every 10 base-pairs (detailed information concerning the variation of these structural parameters with base-pair sequence can be found in the book by W. Saenger[1]). The hard-core diameter of the double helix is about 25 Å (although in solution the phosphates become negatively charged and electrostatic effects tend to increase the DNA's effective diameter). Normally, the hydrophobic purines and pyrimidines are at the core of the double helix, and the hydrophilic phosphate-sugar backbone winds around the outside of the molecule (Fig. 1(C)). The stacking of the planar base-pairs one on top of the other and the electrostatic repulsion between phosphate groups contribute to making DNA a relatively stiff molecule.

Thus in regular DNA the letters of the genetic code tend to be hidden from the molecule's environment. This poses a problem for the polymerase enzymes whose role it is to read the genetic code and use it as a template for de novo synthesis of a complementary strand (as in the case of DNA replication or transcription). These polymerases can only read the code if the bases are exposed to the environment. Unwinding the DNA molecule therefore appears as a way to mechanically separate the two strands of the double helix and make the genetic code accessible. DNA unwinding or negative supercoiling, was first discovered in 1965 by Vinograd and coworkers in small circular DNAs[2] (plasmids). Research has since shown that in practically all living cells DNA is slightly unwound relative to its natural, torsionally relaxed form (certain archaeabacteria, which seem to maintain their DNA in an overwound state, are an interesting exception[3]).

B. DNA Topology

The topology of all DNA molecules can be described by three simple quantities.[4, 5] The first is the twist (Tw), the number of helical turns along the molecule. For torsionally unconstrained B-DNA, $Tw = Tw_0 = N/h$ where N is the number of bases and $h = 10.4$ is the number of bases per turn of the helix. The second topological quantity of interest is the writhe (Wr) of the molecule. Writhing may be easily visualized on a twisted phone

cord, where the formation of interwound structures, known as plectonemes, appears as a way to relax twist strain introduced at the handset. In these structures the number of times the cord loops over itself is its writhing number, and a positive or negative value may be assigned to it. The writhe represents the wrapping of the molecule's axis with itself. If the DNA molecule is torsionally constrained, then the total number of times that the two strands of the helix cross each other (either by twist or writhe) is a topological invariant of the system called the linking number $Lk = Tw + Wr$.[4] Rotating one end of a linear DNA molecule is one way to access and modify Lk:

$$\Delta Lk = Lk - Lk_0 = \Delta Tw + Wr \tag{1}$$

where the linking number of a torsionally relaxed DNA is written as $Lk_0 = Tw_0 + Wr_0$ and $\Delta Tw = Tw - Tw_0$. Assuming that DNA has no significant spontaneous curvature with which it could form coils or loops, $Wr_0 = 0$. The relative difference in linking number between the supercoiled and relaxed forms of DNA is called the degree of supercoiling, σ:

$$\sigma = \frac{Lk - Lk_0}{Lk_0} \tag{2}$$

One uses σ to compare the supercoiling of molecules with different lengths. The molecule is overwound when σ is positive, underwound when it is negative. DNA *in vivo* is typically unwound to $\sigma \sim -0.06$. For DNA to be torsionally constrained, two conditions must be fulfilled: there can be no breaks ("nicks") in either of the molecule's sugar-phosphate backbones, and the rotation of the ends must be blocked. Unnicked circular DNAs can be supercoiled since in this case the molecule's ends are blocked by being joined together.

C. Biological Relevance of DNA Supercoiling and Methods of Investigation

Although supercoiling was first identified in plasmids, a linear DNA molecule may also be torsionally constrained if it is anchored at several points to a physical support, either by its extremities or along its length. For example, it is believed that each eukaryotic chromosome contains a single long DNA molecule anchored every 50,000 base-pairs or so to a dense protein scaffold (this scaffold gives metaphase chromosomes their characteristic X-shape).[6] Each anchor region delimits a topologically constrained section of the chromosomal DNA. Additionally, DNA in chromosomes is solenoidally wrapped around the histone protein complex (roughly -2 turns

per histone) every 200 base-pairs or so.[7] DNA supercoiling is thus implicated in processes ranging from DNA packaging (responsible for fitting 3 meters of DNA into the cell nucleus which has a $\sim 10\ \mu$m diameter)[8] to DNA transcription[9–11] and DNA recombination (the swapping of segments which takes place between DNA molecules to enhance genetic diversity).[12] X-ray crystallography data show that many proteins and enzymes which interact with DNA do so by generating local deformations such as bending and unwinding.[13] A class of enzymes which regulates supercoiling *in vivo*, the topoisomerases,[14] has been identified and even selected as a target within cancerous cells. Indeed, cells deficient in functional topoisomerase II (responsible for unknotting DNA catenanes) cannot proceed normally through cell division. If the freshly-duplicated chromosomes destined to be divided between two daughter cells are not unknotted, they undergo spectacular fragmentation as a result of a powerful cellular "tug of war."

DNA supercoiling is thus extensively studied because it relates the molecule's biological activity to its topology and not just its sequence. Over the course of the years, many techniques have been developed by biologists and physicists to investigate DNA supercoiling. Early cryo-electron microscopy of circular,[2] supercoiled molecules showed that such molecules assume compact, interwound forms much like a twisted phone cord. Gel electrophoresis[15] and sedimentation techniques[16] exploit this compact aspect of supercoiled DNA to separate molecules with different degrees of coiling. Gel electrophoresis consists in forcing a sample of DNA molecules (negatively charged in solution) to migrate through a reticulated gel (such as agarose or polyacrylamide) under the influence of an electric field. Bulkier DNA molecules migrate at slower rates through the gel, allowing for size fractionation of the molecules. Since the compaction of DNA increases with its supercoiling, gel electrophoresis can be used to separate molecules of the same length but with different degrees of supercoiling. Although these techniques have yielded a wealth of information, they have several limitations. First of all, they do not allow for real-time observation of DNA-protein interactions. Secondly, enzymatic and chemical reactions which generate supercoiling produce statistical distributions of topoisomers rather than a single population. Finally, these reactions are not easily reversed after observation and can only yield molecules with roughly $-0.1 < \sigma < 0.1$.

Recent advances in micromanipulation techniques now enable researchers to go one step further and perform controlled, reversible experiments on individual DNA molecules.[17–19] On one hand, biologists are keen to learn more about the mechanical forces involved in DNA processing and the influence of the molecule's topology on its function. On the other hand, micromanipulation experiments are of fundamental interest to

polymer physicists because the size, monodispersity, relative stiffness and ease of handling of DNA combine to make it an excellent system on which to test theories of polymer relaxation,[20] reptation,[21] and elasticity.[17] Notice however that the topological strand interlinkage property of double-stranded DNA is essentially unique among polymers. Mutations aside, the monodispersity of a species' genetic code is vital: all DNA molecules extracted from the bacteriophage-λ (a virus which infects *E.coli*) are exactly 48502 base-pairs long (16.2 μm). Moreover, molecular biologists have at their disposal an arsenal of enzymes capable of catalyzing sequence-specific reactions which include cleaving DNA (restriction enzymes), re-ligating DNA (ligases), polymerizing DNA (polymerases) and labeling DNA with various biochemical groups. Such groups are effective "handles" which allow one to physically grasp the molecule (see Fig. 4). Finally, DNA can also be visualized[22] using the fluorescence of dye molecules (ethidium bromide, YOYO1, and TOTO1 are but a few) which insert themselves ("intercalate") between the planar base-pairs.

In the experiments we will present in this paper, a modified (16.9 μm-long) λ-DNA molecule is biochemically bound at one end to a glass surface and at the other end to a small magnetic bead. The magnetic bead can then be pulled on and forced to rotate using a magnetic field, allowing us to stretch and to wind the molecule in a quantitative, reversible fashion. Using videomicroscopy to observe and analyze the Brownian motion of the magnetic bead one may determine the stretching force applied to it and the molecule's resulting extension. Micromanipulation techniques of this sort are important because they allow one to control the constraints applied to the molecule in a way that is not possible using standard, bulk-phase molecular biology techniques. For example, our system enables us to over- and under-wind the DNA to levels which are impossible to attain using biochemical means. Another important point is that constraints applied by mechanical means are quickly and easily reversed, which is not always the case for biochemically-generated constraints. We find in our experiments that DNA can be repeatedly and vigorously supercoiled, and this without "fatigue." Finally, by coupling observation and micro-manipulation these experiments bring us closer to real-time observation of individual molecular events.

II. DNA MICROMANIPULATION TECHNIQUES

In general, DNA micromanipulation techniques involve the strategy described above. Biochemical handles are attached to the ends of a DNA molecule and serve as anchoring points to manipulable, physical supports. Steve Smith and coworkers performed the first DNA micromanipulation

experiments on torsionally unconstrained DNA.[17] They attached individual DNA molecules by one end to a glass surface and by the other to a small magnetic bead, and used a combination of hydrodynamic flows and magnetic fields to calibrate and apply stretching forces between 10 fN and 20 pN to the DNA. In another scheme,[18] the DNA was bound at one end to a glass surface via an active polymerase enzyme and at the other to a small polystyrene bead which was acted upon by an optical trap. This setup allowed Yin *et al.*[18] to measure the stall-force of the *E. Coli* RNA polymerase, $\sim 15pN$. The optical trap (used in other experiments to cool and trap atoms[23]) can be generated by focusing a laser beam within the sample using a high aperture (N.A. = 1.4) oil-immersion microscope lens. If the bead is of the appropriate dimensions, does not absorb the radiation and has an index of refraction higher than that of the aqueous solution in which the experiment is performed, it tends to be confined in the three spatial directions at the laser's focal point. The trap stiffness can be calibrated by applying a controlled hydrodynamic flow to a trapped bead and measuring its displacement within the trap. The laser trap typically generates forces between 100 fN and 50 pN, and multi-laser traps can be used to increase the force range. In the technique used by P. Cluzel and coworkers,[24] the molecule is attached to the tip of a thin glass pipette which can be used to pull on the molecule. As one pulls on the molecule, the deflection of the micropipette tip can be measured to obtain the applied force. Again, the stiffness of the glass micropipette must be calibrated against a standard glass fibre. This technique does not give precise measurements below the pN range but can be used to apply forces in excess of 100 pN. In the technique we describe in this paper, a magnetic bead is acted upon by a magnetic force. The magnitude of the force (from a few fN to about 100 pN) is determined by measuring the amplitude of the bead's Brownian fluctuations; besides being non-invasive, this technique has the advantage of requiring no previous force calibrations.

III. DNA STRETCHING EXPERIMENTS

There are two main regimes in the elasticity of linear polymers such as DNA: a low-force regime where entropic elasticity dominates, and a high-force regime where the molecule is fully extended and its chemical bonds are deformed. When DNA is left unstretched, it is in a "compact" random-coil conformation which allows it to maximize its entropy. As one increases the stretching force the distance between the ends of the molecule begins to increase; the random coil becomes biased and the system's entropy begins to decline.[25] Typically, the random coil is noticeably deformed for a force

$F \sim k_B T/\xi$, where $k_B T \sim 4.10^{-21}$ J is the thermal energy and ξ represents the characteristic length-scale of orientational fluctuations (or persistence length) of the polymer. Thus DNA, with $\xi \sim 50$ nm, can be partially extended by a force of ~ 0.08 pN. At high stretching forces ($F \sim 10$ pN), the molecule is almost fully extended and its entropy almost fully repressed. When one tugs on this extended molecule, the chemical bonds which make up the molecule are stretched; this is the regime of "enthalpic elasticity." Thanks to micro-manipulation techniques, the cross-over between these two regimes in the case of DNA has been characterized and theoretically modeled.

The basic model of a polymer chain of contour length L is the so-called Kratky–Porod model.[26] It consists of a discretization of the chain by N segments of size b ($=$L/N), orientation unit vector $\hat{t}_i$ and stiffness $k_B T \cdot K$. When stretched by a force $F\hat{z}$ the energy of the chain is

$$\frac{E}{k_B T} = -K \sum_i \vec{t}_i \cdot \vec{t}_{i+1} - \frac{Fb}{k_B T} \sum_i \vec{t}_i \cdot \hat{z} \tag{3}$$

One notices the well-known analogy with a one-dimensional chain of vector spins.[27] In the simplest approximation one neglects the bending energy term (setting the ferromagnetic coupling $K = 0$), thereby assuming the stretching of each segment to be independent ($b = \xi$). The resulting model, the Freely Jointed Chain (FJC) model, is equivalent to an ensemble of paramagnetic spins in a field and its relative extension l/L (the mean magnetization) is given by the Langevin function $\mathcal{L}(x) \equiv \coth(x) - 1/x$.

$$\frac{l}{L} = \mathcal{L}\left(\frac{F\xi}{k_B T}\right) \tag{4}$$

The data obtained by Smith *et al.*[17] clearly invalidated the FJC model as a reasonable description of a stretched polymer (see Fig. 2). J. Marko and E. Siggia then analyzed[28] the more realistic continuum limit of Eq. (3): $b \to 0$ ($K = \xi/b$):

$$\frac{E_{WLC}}{k_B T} = \frac{\xi}{2} \int_0^L \left(\frac{d\vec{t}}{ds}\right)^2 ds - \frac{F}{k_B T} \int_0^L \vec{t} \cdot \hat{z}\, ds \tag{5}$$

The partition function of this Worm-Like Chain (WLC) model is similar to the propagator of a quantum dipole in an electric field. In the thermodynamic limit, the free energy of this model is determined by the ground state of the quantum mechanical problem. The derivative of that energy

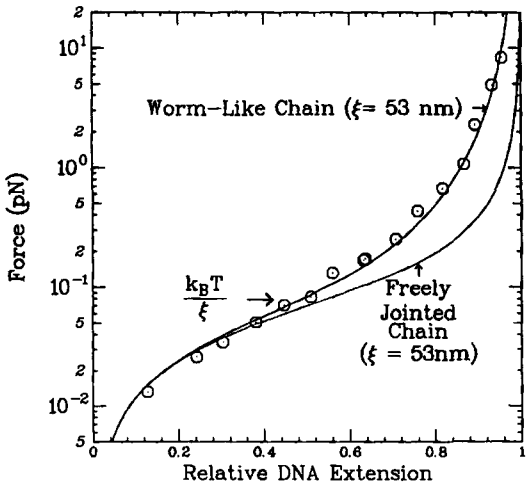

Fig. 2. A comparison of the force versus extension behavior of the Freely-Jointed Chain (FJC) and the Worm-Like Chain (WLC). The relative extension is the length to which the molecule is stretched l divided by its contour length L. Although both models yield the same low-force behavior, the WLC provides a better fit to the experimental data (represented by circles). At a force of $k_B T/\xi \sim 0.08$ pN the DNA is extended by about 50%.

with respect to the force F yields a force versus extension relation which can be written as

$$\frac{F\xi}{k_B T} = \frac{1}{4}\left[\left(1-\frac{l}{L}\right)^{-2} - 1\right] + \frac{l}{L} + \sum_{i=2} a_i \left(\frac{l}{L}\right)^i \tag{6}$$

The first three terms, given by Marko and Siggia[28] yield the correct asymptotical behavior when $l/L \to 0$ and $l/L \to 1$. At low stretching forces this reduces to the random walk with linear elasticity: $F = \frac{3}{2} k_B T/\xi \; l/L$, where l/L is the walk's relative extension. At high forces, the molecule's extension tends towards its contour length according to $l/L \sim (1 - 1/\sqrt{F\xi/k_B T})$. The corrections to this behavior cannot be neglected in the analysis of the high-precision elasticity measurements on single molecules currently possible.[29, 30]

Thus by fitting the WLC model's solution to the experimental data, one can extract the persistence length and the contour length of the system being stretched. Force-extension measurements on DNA appear to be a very precise method for determining the molecule's persistence length. The persistence length of DNA in moderate ionic conditions (10 mM monovalent cations) is 53 ± 3 nm.[28, 31, 30] When one lowers the concentration of cations, the negatively-charged phosphates experience less counterion screening and neighboring phosphates repel each other more strongly. This

leads to an increase in the persistence length. Note that if one is stretching a bead tethered by two DNA molecules (equivalent to two parallel springs) the applied force needs to be doubled to obtain the same extension as for a singly-connected bead. Thus the force-extension data for such a system may be fitted by the WLC model using $\xi \sim 25$ nm. This is an effective way of determining if the stretching force is being applied to one or two DNA molecules (see Fig. 9), a rather critical parameter with regards to DNA supercoiling experiments. In our experiments we can thus distinguish between DNA supercoiling (one DNA molecule) and DNA braiding (two DNA molecules).

So far, we have only discussed stretching regimes (typically $F < 10$ pN) in which the DNA was not strongly deformed. The elastic modulus (stiffness multiplied by length) of DNA, estimated to be between 500 and 1000 pN, has been determined by analyzing force-extension data in the range of 10 to 50 pN.[31, 32] In this range, the increase in length of the DNA is due to the slight distortion of its double-helical structure. At a stretching force of about 65 pN however, the double helix becomes completely disrupted and the molecule's extension abruptly increases to a state 1.7 times its contour length.[33, 24] Molecular modeling[24, 34] of this cooperative transition indicate that the DNA assumes a new structure called S-DNA. Depending on precisely how the molecule is stretched, two possible structures were proposed (1) a ladder (2) a double-helical structure with bases tilted with respect to the helix axis. Such structures could be related to the form assumed by DNA when it is associated with the recA-type proteins which mediate genetic recombination.[12] Theoretical work[35] predicts that the onset and evolution of the B to S transition depends on the DNA backbone's integrity and preliminary experimental results confirm that a lower force is required to generate overstretched DNA if the backbone is nicked than if it is intact.

IV. DNA SUPERCOILING EXPERIMENTS: MATERIALS AND TECHNIQUES

A. DNA Construction and Experimental Setup

The DNA we micromanipulate is the genome of the bacteriophage-λ, 48502 base-pairs long. In order to torsionally constrain this linear DNA molecule, we bind it by its extremities to two physical supports (see Fig. 4). The binding is achieved via two sets of noncovalent biochemical ligand-receptor couples, the biotin-streptavidin and digoxigenin-antidigoxigenin groups. One end of the DNA, labeled with biotin molecules, binds to a small magnetic bead coated with streptavidin. The other extremity of the

molecule is labeled with digoxigenin and binds to the anti-digoxigenin coated glass surface. The key to the construction is that there are multiple bonds between the DNA and each of the supports, as an individual biotin or digoxigenin has a singly-bonded backbone and can thus act as a point of free rotation about which the molecule can release its torsion.

This DNA construction is generated in two stages using standard molecular biology techniques[36] (see Fig. 3). In the first stage, we prepare short ($\sim$1 kb) DNA fragments bearing either digoxigenin or biotin groups. This reaction, known as "labeling," can be accomplished by covalently linking these groups to a pre-existing DNA molecule via photochemical reactions. A gentler approach consists in binding digoxigenin or biotin to nucleotides (typically dUTP) which will then be incorporated into a new DNA molecule during the course of a controlled polymerizing reaction such as the Polymerase Chain Reaction (PCR). The PCR[37] is a powerful technique in which the two strands of DNA are thermally separated before serving as the templates for the polymerization of their complementary strands. The number of DNA molecules thus doubles at each step, and repeating the step $\sim$25 times yields large quantities (e.g., several micrograms) of DNA. After the labeling, the excess in modified nucleotides is

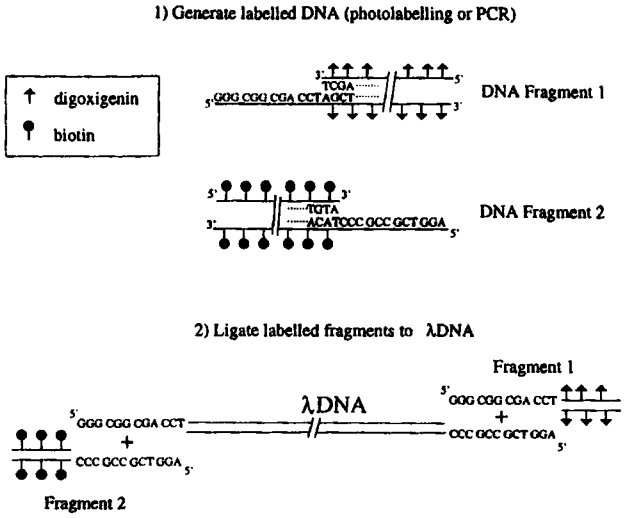

Fig. 3. A brief description of the DNA construction. In the first stage, one generates DNA fragments bearing biotin or digoxigenin "labels." In the second stage, these fragments are covalently attached to λ-DNA thanks to the presence of complementary end sequences and a special enzyme, DNA ligase.

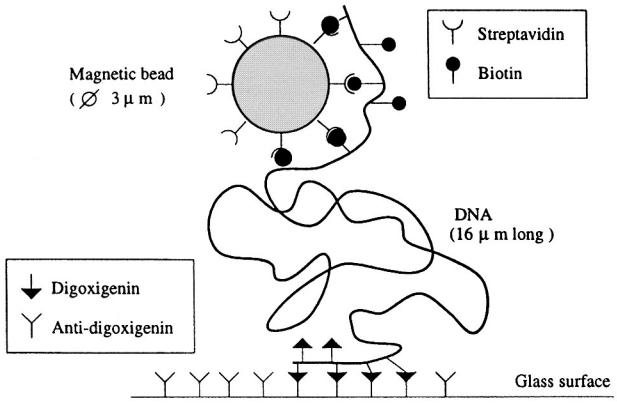

Fig. 4. First, the biotin-labeled end of the DNA construction is bound specifically to a streptavidin-coated magnetic bead. This assembly is then deposited onto a glass surface coated with anti-digoxigenin. The DNA's digoxigenin-coated extremity then binds to the surface. Multiple anchoring sites at each of the two physical supports ensures that the molecule is torsionally constrained.

eliminated using gel electrophoresis or special silica substrates which reversibly bind DNA but not nucleotides.

In the second step, a biotin-labeled fragment must be affixed to one end of the DNA we wish to micromanipulate and a digoxigenin-labeled fragment anchored to the other end of the DNA. This reaction is catalyzed by an enzyme known as ligase, which reconstitutes a phospho-diester bond between neighboring bases by hydrolyzing ATP (adenosine triphosphate, the cell's energy source). In the case of λ-DNA, this step is simplified by the fact that the DNA's extremities are uneven and present a 12 base-pair overhang at the 5' end of each strand (see Fig. 3). By making sure the labeled fragments have at one end the sequence complementary to one of these overhangs, base-pairing interactions between the two molecules will hold them together ("anneal") while ligase covalently links them. Typically, we thus anneal and ligate the biotin-labeled fragment to the left end of the λ-DNA and then anneal and ligate the digoxigenin-labeled fragment to the right end of the λ-DNA. The final construction contains roughly 50.5 kbp, 2 kbp of which are labeled, giving a crystallographic length $l_o \sim 16.9$ μm.

The construction is first bound to the magnetic beads in the bulk before being pipetted and deposited on the glass surface. The glass surface is actually the inner "floor" of a square capillary tube; the beads settle to its surface, where the DNA may then anchor by its second extremity. The capillary is attached to a buffer-flow system, allowing us to change the ionic conditions of the experiment, add or remove enzymes, and so on. The

tube is also in thermal contact with a copper support, the temperature of which is controlled in the range of 16 Celsius to 65 Celsius via Peltier modules and a feedback loop. As represented in Fig. 5, the sample rests atop a 60x oil-immersion lens mounted on an inverted microscope. A CCD camera relays the image as generated by the lens to a PC. By placing a pair of magnets focused by polar pieces over the sample, we generate a magnetic field whose axis is horizontal but whose gradient is vertical. Thus, the superparamagnetic bead's induced magnetic dipole will align with the field axis. At the same time, the dipole causes the bead to be pulled along the field gradient towards increasing fields. The vertical force felt by the bead increases when we bring the magnets closer to the sample and decreases if we move them away. The magnets are mounted on a translation stage which allows us to relate the applied force to the vertical distance between the magnets and the sample. If the magnets are made to rotate, a very strong torque is applied to the bead via its dipole moment and the bead turns synchronously with the magnets. This forces the molecule to coil, allowing us to modify its linking number Lk. Thus, the magnets make it possible to rotate the bead by a fixed number of turns and to pull on it with a magnetic force.

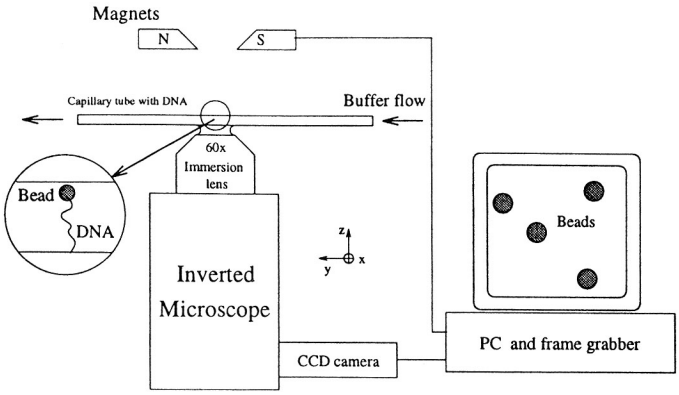

Fig. 5. An overview of the experimental setup. Experiments are carried out in a glass capillary tube (1 mm × 1 mm × 50 mm) functionnalized with anti-digoxigenin. Not shown are the buffer flow system (which allows us to change the ionic conditions of the experiment and add enzymes) and the thermal regulation unit (used to regulate the temperature of the capillary). The tube rests atop a 60X oil-immersion lens mounted on an inverted microscope. A CCD camera operating at 25 Hz relays the images of the magnetic bead to a PC. The magnetic field used to manipulate the bead is generated by two magnets fitted with pole pieces. The rotation of these magnets, as well as their vertical distance from the sample, is controlled by the PC.

B. Force Measurement Technique

Since measuring this magnetic force would require characterizing the field as well as the bead's susceptibility, we have developed a simpler technique based on an analysis of the bead's Brownian motion. The PC applies a real-time tracking algorithm to the video data it receives in order to determine the Brownian motion of the magnetic bead in the microscope's focal plane as well as perpendicular to the focal plane (this is achieved by following the apparent fluctuations of the diffraction rings of the bead). The relative displacements of the bead in the x, y and z directions can be obtained to within 10 nm. Thus, the average position of the bead, as well as its Brownian fluctuations, can be obtained simultaneously along the

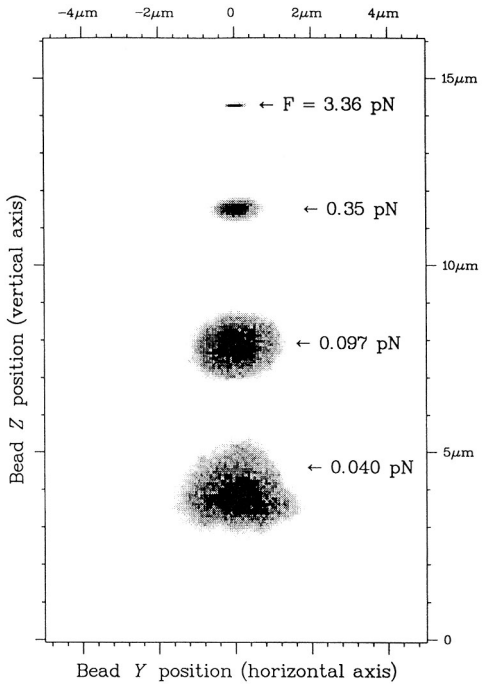

Fig. 6. Plots of the bead's Brownian motion for several different stretching forces. The cloud of points represents the positions of the bead's center during the data acquisition along the y (horizontal) and z (vertical) directions, as if the bead were being viewed from the side. Although motion along the x-direction is not shown, it is essentially isotropic with regards to the y-motion. At low forces, the bead's motion along all three axis is isotropic and covers displacements of up to a few microns from the mean position. As the stretching force increases, motion along the y and z axes becomes progressively more restricted. At higher forces ($F \sim 3$ pN) the molecule nears full extension and the motion along the z-axis decreases as the molecule's rigidity increases.

three spatial directions. An example of the raw data can be found in Fig. 6. The DNA-bead system essentially behaves like a small pendulum pulled to the vertical of its anchoring point and subjected to Brownian fluctuations, see Fig. 7. The vertical stretching force F may be expressed as

$$F = \frac{k_B T l}{\langle \delta x^2 \rangle} \tag{7}$$

where l is the molecule's extension (not to be confused with its contour length L) and $\langle \delta x^2 \rangle$ is the mean square of the bead's fluctuations along the x-direction (transverse to the molecule's axis). Thus, a force measurement can be performed by measuring lengths, requiring no further force calibrations (as opposed to techniques based on optical tweezers,[31, 33] hydrodynamic flows[17] or glass cantilevers[24, 38]). A compendium of force measurements is represented Fig. 8: note that nearly five orders of magnitude in the force may be measured. The forces relevant to stretching DNA are thus well encompassed by this technique, as are those relevant to the processive motion of molecular motors (on the order of 10 pN[18]). The main disadvantage of this technique is that the acquisition time increases as the force decreases (since one must give the bead time to statistically sample the space available to it in order to correctly determine $\langle \delta x^2 \rangle$).

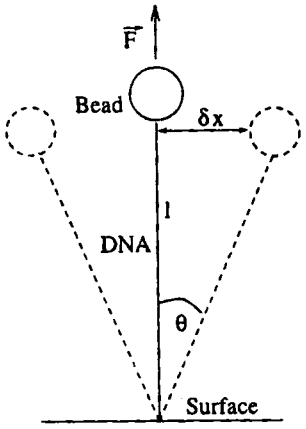

Fig. 7. The stretched bead-DNA system may be analyzed as a small pendulum. A vertical stretching force F applied to the bead acts to extend the molecule to a length l. The bead is buffeted by the Brownian motion of the water molecules, displacing it a distance δx from its equilibrium position. A restoring force approximately equal to $F\theta \sim F/l\,\delta x$ acts to bring the bead back to the vertical of its anchoring point. F/l is the effective stiffness of the pendulum in the x-direction. According to the equipartition theorem, the pendulum's energy along the x direction is $\frac{1}{2}F/l\langle \delta x \rangle^2 = \frac{1}{2}k_B T$. Therefore, $F = k_B T l/\langle \delta x^2 \rangle$.

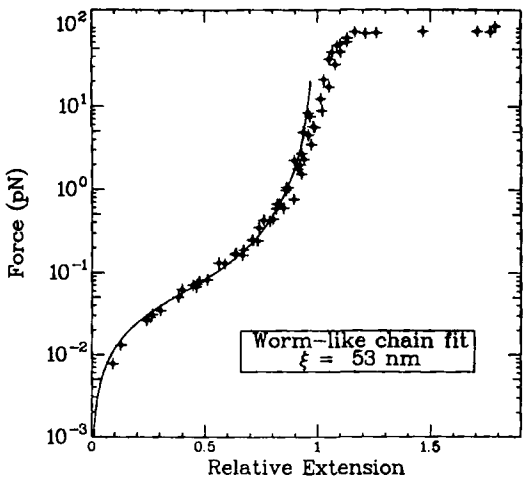

Fig. 8. A compendium of force measurements on different DNA molecules (normalized relative to their contour length). Forces as low as 6 femtoNewtons and as high as 100 picoNewtons can be applied and measured in our experimental setup. The solid line corresponds to the Worm-Like Chain fit to the portion of the data where the relative extension is less than one. At a force of about 70 picoNewtons the molecule undergoes an abrupt transition to the so-called S-form (for stretched), where its extension is about 1.7 times that of the B-form.

To give an idea of the time required to obtain an accurate force measurement, we consider the characteristic time-scale τ of the system's fluctuations along the x-axis. This is simply the inverse of its cutoff frequency: $2\pi/\tau_c = \omega_c = 6\pi\eta r/(F/l)$, where η is the viscosity and r the bead radius. Then by waiting a time T, the relative statistical error ε on the force measurement will be equal to $1/\sqrt{T/\tau}$. In the enthalpic force regime ($5pN < F < 25pN$), the DNA's length is basically constant and roughly equal to its crystallographic length l_0, so that $T = 12\pi^2\eta r l_0/F\varepsilon^2$. So to measure a 5 pN force to within 10% on a DNA extended by 16 μm via a 3 μm bead requires just over a minute.

At low DNA extensions, $F/l = \frac{3}{2}k_B T/\xi l_0$ and so $T = 8\pi^2\eta r\xi l_0/k_B T\varepsilon^2$. In this case, 10% accuracy on the force is achieved after a $\sim$40 minute acquisition. If one keeps the acquisition time constant at 40 minutes while increasing the force, a maximum statistical error of 10% on the force measurement is guaranteed (an explicit expression for intermediate forces can be obtained by replacing F by Marko and Siggia's interpolation formula). Since the force measurements take a while, we begin the experiments by measuring the force applied to a particular bead as a function of the magnets' height above the sample. Once this time consuming force

measurement is completed, we simply adjust the magnets' height to generate the desired force.

V. RESULTS

A. Results on Torsionally Relaxed DNA

Since the anchoring step between DNA and magnetic bead takes place in the bulk, it is possible to end up with a bead bound to the surface by multiple molecules. It is therefore crucial to begin by determining the number of molecules one is stretching. As mentioned earlier, this can be accomplished by measuring the force versus extension diagram of the bead/DNA system and fitting the WLC model to the data. By extracting its effective persistence length, one is able to determine the number of tethering molecules. In Fig. 9, we plot the force versus extension data for three different systems: a bead bound by a single 16 μm-long DNA, a bead bound by two 16 μm-long DNA and a bead bound by one 16 μm-long DNA and one 32 μm-long DNA. The worm-like chain fits to these three data sets yield persistence lengths of 53, 26 and 44 nanometers, respectively.

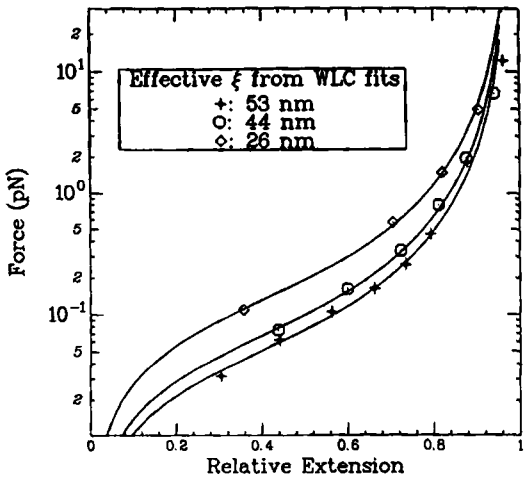

Fig. 9. Force versus extension carves and worm-like chain fits for three different systems. A single DNA molecule of contour length $l_o = 16$ μm has a persistence length of 53 nm and a system comprised of two molecules of contour length l behaves like a polymer with a 26 nm persistence length. A two molecule-system comprised of a molecule of length l and a second of length $2l$ displays an effective persistence length of 44 nm.

B. Results on Torsionally Stressed DNA

1. Extension versus Supercoiling Measurements at Constant Force. Two types of experiments are possible once a single-molecule system is identified. We may set and hold the supercoiling constant and measure the system's force-extension diagram, or we may measure the molecule's extension as a function of supercoiling while maintaining a constant stretching force. We begin by presenting results of the latter type in Fig. 10. Once again, it is important to point out that these experiments are all fully reversible in terms of both force and degree of supercoiling.

These experiments were performed at room temperature in an aqueous solution containing 10 mM phosphate cations (pH 8). When the DNA is subjected to a weak stretching force ($F = 0.1$ pN), its extension versus supercoiling behavior is symmetric with respect to the sign of the supercoiling. In both cases, the molecule contracts at a constant rate of about 0.08 μm per turn. When the stretching force is increased to $F = 1$ pN, the symmetric behavior breaks down and the molecule only contracts when it is positively supercoiled. When the molecule is negatively supercoiled, its extension does not vary noticeably in the range of supercoiling depicted here. If the force is further increased to a value of 8 pN, then the molecule's extension becomes nearly insensitive to both positive and negative supercoiling.

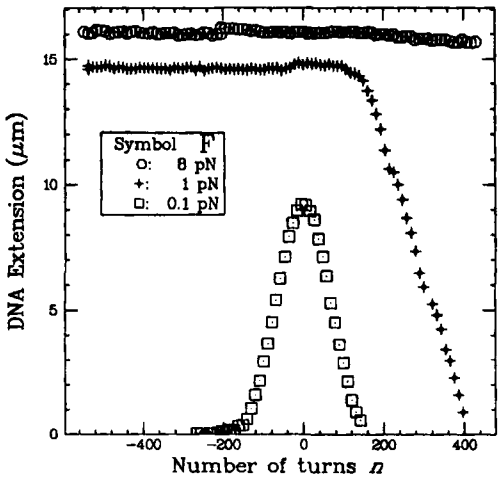

Fig. 10. Extension versus supercoiling curves. The stretching force applied to the molecule is held constant while the bead is rotated one way or the other. The experiments were carried out in the presence of 10 mM phosphate cations and at room temperature.

2. Force versus Extension Curves at Constant Degree of Supercoiling. The previous section therefore indicates that there are three regimes in the extension versus supercoiling behavior of DNA. These three regimes are also evident in the force versus extension curves obtained at constant supercoiling (Fig. 11). These curves are generated by rotating the DNA by the desired amount and then measuring its extension as the force is varied. For both positive and negative supercoiling, the molecule's rigidity increases very rapidly under the action of coiling. Indeed, the DNA's elasticity is sensitive to as low as a 1% change in the molecule's degree of supercoiling. The second point of interest is that, for negative as well as for positive supercoiling there appears a critical force above which the DNA's extension abruptly increases and the force-extension diagram nearly rejoins that of the torsionally relaxed DNA.

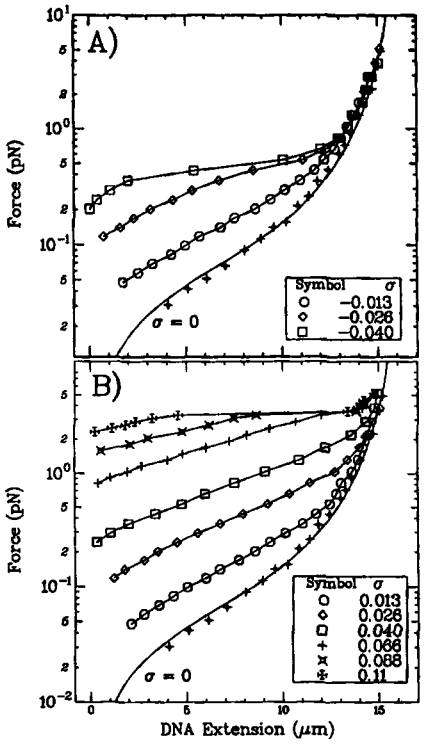

Fig. 11. Force versus extension curves (at fixed degree of supercoiling). These curves were obtained in the same conditions as in Fig. 10. (A) Negatively supercoiled DNA and (B) Positively supercoiled DNA.

In the ionic conditions presented here the critical force for unwound DNA $F_c^- \sim 0.3$ pN, while for positively supercoiled DNA $F_c^+ \sim 3$ pN, an order of magnitude greater. The existence of these transitions explains the three regimes described in the previous section. For $F = 0.1$ pN $< F_c^- < F_c^+$, the DNA's extension varies with the degree of supercoiling; this constitutes the first regime described above. For $F_c^- < F = 1pN < F_c^+$ however, the negatively supercoiled DNA's extension does not change much with σ whereas that of the positively supercoiled DNA may still vary. Finally, when the stretching force is greater than both F_c^- and F_c^+ (as is the case for $F = 8pN$), the molecule's extension is basically independent of the degree of supercoiling.

The critical force F_c^- appears to be independent of the degree of supercoiling for $\sigma < -0.015$. The same is true for F_c^+ when $\sigma > 0.037$. Additional experiments[39] show that the critical forces are lowered when the temperature is increased or when the concentration of cations is decreased. When one increases the concentration in cations, the critical forces increase.

VI. DISCUSSION

A. Interpretation of the Critical Forces

Biochemical studies indicate that DNA under physiological degrees of supercoiling may denature at the base-pair scale to alleviate its torque.[40–42] By examining a simple mechanical model such as a twisted phone cord, one may see that at low forces the unwinding is stored in writhed structures. As the stretching force is increased however, the plectonemes are destabilized and the linking number deficit must be stored by negatively twisting the system's axis. It is believed that negatively supercoiled DNA cannot change its twist by more than $-\sim 1\%$ to accommodate a linking number deficit.[40, 43] We therefore propose that as one stretches an unwound molecule the abrupt lengthening that occurs at F_c^- is related to the formation of a denaturation bubble (where the base-pairing, and thus the double-helix, is destroyed) in the molecule. Simultaneously, the plectonemes disappear since the linking number deficit is absorbed by the bubble. Thus the molecule's extension increases. In other words, as the molecule is stretched and writhe is transformed into twist the torque acting on the molecule's axis builds up; beyond a certain value (attained at the critical force) the strands are forced to locally unravel and separate. Since the twist of the denatured region is essentially zero, the remainder of the molecule may then adopt a B-form conformation free of writhing. If the denaturation bubble is small enough, the extension of the DNA will be almost identical to that of the torsionally relaxed molecule.

We estimate that the torsional stress Γ which acts on the molecule grows as:

$$\Gamma = \frac{k_B T}{l_0} C \times 2\pi \, \Delta Tw \tag{8}$$

where $C \sim 75$ nm is the DNA torsional stiffness and l_o its contour length. Biologists estimate that plasmids (naturally unstretched, $F = 0$) begin to locally denature at roughly $\sigma = -0.07$, and have a $Wr/\Delta Tw \sim 4$, placing the critical torque energy beyond which negatively supercoiled DNA denatures at roughly $\Gamma_c^- \sim k_B T = 4$ pN · nm. A similar argument can be made for the transition observed at F_c^+, in which the molecule's overwinding is stored in local regions with a strong helical pitch. Since F_c^+ is roughly an order of magnitude greater than F_c^-, the critical torsion energy is also ten times greater for overwound DNA. We therefore estimate that for overwound DNA ΔTw_c will be about 3 times greater than for unwound DNA, or about 3%.

B. Comparison with Theoretical Results on Stretched Coiled DNA

The theory of stretched supercoiled DNA in the force regime we study here has been developed by J. Marko and E. Siggia.[44, 45] Here we shall briefly describe their arguments and compare their predictions with our results.

To obtain the energy E for stretching a coiled DNA, one must add a twist energy term to Eq. 5[45]

$$\frac{E}{k_B T} = \frac{E_{WLC}}{k_B T} + \frac{C}{2} \int_0^L \Omega^2(s) \, ds \tag{9}$$

where $C \sim 75$ nm[45] is the persistence length for torsion and $\Omega(s)$ the local change in the twist rate ω_0 ($= 2\pi/h_0 = 1.85$ nm^{-1} for B-DNA with a pitch $h_0 = 3.4$ nm). It is far from trivial to obtain the partition function of this system, in particular in the presence of self-avoidance which is necessary to prevent the torsional relaxation inherent to a phantom chain. Marko and Siggia have simplified the problem by calculating the free energy of two particular configurations. The first is the plectonemic supercoil whose free energy depends only on its degree of supercoiling σ_p: $\mathscr{E}_p(\sigma_p)$. The other is a stretched solenoidal supercoil whose free energy depends on the force F and degree of supercoiling σ_s: $\mathscr{E}_s(F, \sigma_s)$. They then assume that a supercoiled DNA under tension will contain a fraction p of plectonemic domains

and $1-p$ of stretched solenoidal domains. The molecule's free energy then becomes:

$$\mathscr{E} = p\mathscr{E}_p(\sigma_p) + (1-p)\,\mathscr{E}_s(F, \sigma_s) \tag{10}$$

while the degree of supercoiling breaks down according to

$$\sigma = p\sigma_p + (1-p)\,\sigma_s \tag{11}$$

By numerically minimizing the molecule's free energy $\mathscr{E}$ with respect to p and σ_p, the DNA's extension can be determined:

$$l = -\frac{\partial \mathscr{E}_{min}(F, \sigma)}{\partial F} \tag{12}$$

Because the DNA's energy, Eq. (9) is symmetric under $\Omega \rightarrow -\Omega$ that approach predicts extensions which are identical for σ and $-\sigma$. One might thus expect its results to apply in the low force regime. Unfortunately in this low force, low extension (and low σ) regime, the assumptions made[45] are uncontrolled. Moreover to describe the abrupt transitions at F_c^- and F_c^+ one has to introduce the existence of alternative DNA structures (see below) for values of σ_p greater than some arbitrary thresholds.

In spite of these shortcomings, the theoretical results are in agreement with our measurements.[46] This is particularly true for $0.01 < \sigma < 0.1$, in a range where we see no abrupt transitions in the force vs. extension curves and where one might expect Marko and Siggia's approach to be valid with no ad-hoc assumptions on the appearance of alternative DNA structures. A more detailed approach to describing small degrees of supercoiling ($|\sigma| < 0.01$) has been proposed by Bouchiat and Mézard[47] and Moroz and Nelson.[48] The partition function of a stretched, twisted thin rod has been calculated using a quantum mechanical analogy with the propagator of a charged particle constrained to move on the unit sphere under the joint action of an electric field and the field of a magnetic monopole.[47] The extension versus supercoiling behavior generated by this model is in good agreement with our data and can be used to determine the ratio of the twist persistence length to the bend persistence length, $C/\xi \sim 1.64$.

C. Biological Relevance of the Structural Transitions Observed

It is interesting to note that the forces and degrees of supercoiling we describe here are likely to exist within the cell nucleus. As mentioned previously, DNA *in vivo* is negatively supercoiled to about $\sigma = -0.06$. Since

the DNA is wrapped around histones, it is believed that the twist in the molecule is effectively null and so is its torque. On the other hand, naked DNA (i.e. not associated to histones) has to partition its linking number deficit between twist and writhe. If that partitioning is 1:4, then the torque on the molecule will be slightly sub-critical, helping to destabilize the molecule. This local destabilization of the double helix has been seen to favor the initiation of DNA transcription.[10] Positively supercoiled DNA is also biologically relevant: it has been identified in archaeobacteria which live in extreme temperature conditions,[3] and it is also seen to arise in regions of the genome which are actively being transcribed. Indeed, *in vivo*[9] studies have shown that as RNA polymerase transcribes DNA into RNA, it generates waves of positive supercoiling which propagate ahead of the transcription complex and a wake of negatively supercoiled DNA behind it. A simple way to visualize this phenomenon is by twisting two strings together and pulling the system taut. By inserting a pencil (which represents the polymerase) at one end between the two strings and pushing it towards the other end, the string overwinds ahead of the pencil and underwinds behind it.

Thus, the degrees of supercoiling we discuss in this article exist in the cell nucleus. The forces we generate in our experimental setup are also accessible to the cell. The transcribing RNA polymerase which we mention in the previous paragraph is capable of working against a load of up to about 15 pN.[18] It can therefore generate forces on the order of 15 pN on chromosomal DNA, in the process disrupting the DNA's packaging around histones. Since the structural transitions we observe occur at forces smaller than 15 pN, we speculate that they may take place within the nuclear context.

VII. CONCLUSION

Micromanipulation techniques enable biophysicists to ask new types of questions: how does the force applied to a macromolecule affect its structure?[49] At what forces will the molecule's function be modified? In the case of DNA we have seen that the interplay of stretching and twisting provokes structural transitions in the molecule which may play a role in the processing of the genetic code. It is important to note that DNA is only the first biological macromolecule to have been studied in such a manner. Having characterized the mechanical response of DNA to supercoiling in a variety of ionic and thermal conditions, it will soon be possible to study the effect of DNA supercoiling on its interactions with proteins such as topoisomerases and histones. Finally, the extension of micromanipulation techniques to molecular motors such as RNA polymerase,[18] F_1-ATPase[50]

(a rotary motor involved in the synthesis of ATP), myosin[51] and kinesins,[52] to name but a few, is certain to bring forth new exciting questions.

REFERENCES

1. W. Saenger, *Principles of Nucleic Acid Structure* (Springer-Verlag, 1988).
2. J. Vinograd, J. Lebowitz, R. Radloff, R. Watson, and P. Laipis, The twisted circular form of polyoma virus DNA, *Proc. Natl. Acad. Sci. (USA)* **53**:1104–1111 (1965).
3. F. Confalonieri, C. Elie, M. Nadal, C. de la Tour, P. Forterre, and M. Duguet, Reverse gyrase: A helicase-like domain and a type I topoisomerase in the same polypeptide, *Proc. Natl. Acad. Sci. (USA)* **90**:4753–4757 (1993).
4. J. H. White, Self-linking and the gauss integral in higher dimensions, *Am. J. Math.* **91**:693–728 (1969).
5. C. R. Calladine and H. R. Drew, *Understanding DNA* (Academic Press, 1992).
6. M. Roberge and S. M. Gasser, DNA loops: Structural and functional properties of scaffold-attached regions, *Molecular Microbiology* **6**:419–423 (1992).
7. J. D. Watson, N. H. Hopkins, J. W. Roberts, J. A. Steitz, and A. M. Weiner, *Molecular Biology of the Gene*, 4th ed. (Benjamin/Cummings Publishing Comp., New York, 1987).
8. H.-G. Patterton and C. von Holt, Negative supercoiling and nucleosome cores. I. The effect of negative supercoiling on the efficiency of nucleosome core formation in vitro, *J. Mol. Biol.* **229**:623–636 (1993).
9. H.-Y. Wu, S. Shyy, J. C. Wang, and L. F. Liu, Transcription generates positively and negatively supercoiled domains in the template, *Cell* **53**:433–440 (1988).
10. M. Dunaway and E. A. Ostrander, Local domains of supercoiling activate a eukaryotic promoter *in vivo*, *Nature* **361**:746–748 (1993).
11. T. Tsukiyama and C. Wu, Chromatin remodeling and transcription, *Curr. Op. Genet. Dev.* **7**:182–191 (1997).
12. A. I. Roca and M. M. Cox, The RecA protein: Structure and function, *Crit. Rev. Biochem. Mol. Biol.* **25**:415–456 (1990).
13. A. Lebrun, Z. Shakked, and R. Lavery, Local DNA stretching mimics the distortion caused by the tata-box binding protein, *Proc. Natl. Acad. Sci. (USA)* **94**:2993–2998 (1997).
14. J. C. Wang, DNA topoisomerases, *Annu. Rev. Biochem.* **65**:635–692 (1996).
15. W. Keller, Determination of the number of superhelical turns in simian virus 40 DNA by gel electrophoresis, *Proc. Natl. Acad. Sci. (USA)* **72**:4876–4880 (1975).
16. V. V. Rybenkov, N. R. Cozzarelli, and A. V. Vologodskii, Probability of DNA knotting and the effective diameter of the DNA double helix, *Proc. Natl. Acad. Sci. (USA)* **90**:5307–5311 (1993).
17. S. B. Smith, L. Finzi, and C. Bustamante, Direct mechanical measurements of the elasticity of single DNA molecules by using magnetic beads, *Science* **258**:1122–1126 (1992).
18. H. Yin, M. D. Wang, K. Svoboda, R. Landick, S. M. Block, and J. Gelles, Transcription against an applied force, *Science* **270**:1653–1656 (1995).
19. T. R. Strick, J.-F. Allemand, D. Bensimon, A. Bensimon, and V. Croquette, The elasticity of a single supercoiled DNA molecule, *Science* **271**:1835–1837 (1996).
20. T. T. Perkins, S. R. Quake, D. E. Smith, and S. Chu, Relaxation of a single DNA molecule observed by optical microscopy, *Science* **264**:822–826 (1994).
21. T. T. Perkins, D. E. Smith, and S. Chu, Direct observation of tube-like motion of a single polymer chain, *Science* **264**:819–822 (1994).

22. A. Bensimon, A. J. Simon, A. Chiffaudel, V. Croquette, F. Heslot, and D. Bensimon, Alignment and sensitive detection of DNA by a moving interface, *Science* **265**:2096–2098 (1994).
23. S. Chu, Laser manipulation of atoms and particles, *Science* **253**:861–866 (1991).
24. P. Cluzel, A. Lebrun, C. Heller, R. Lavery, J.-L. Viovy, D. Chatenay, and F. Caron, DNA: An extensible molecule, *Science* **271**:792–794 (1996).
25. P.-G. de Gennes, *Scaling Concepts in Polymer Physics* (Cornell University Press, 1979).
26. C. R. Cantor and P. R. Schimmel, *Biophysical Chemistry: Part III. The Behavior of Biological Macromolecules* (Freeman, 1980).
27. M. E. Fisher, *Am. J. Phys.* **32**:343 (1964).
28. C. Bustamante, J. F. Marko, E. D. Siggia, and S. Smith, Entropic elasticity of λ-phage DNA, *Science* **265**:1599–1600 (1994).
29. J. F. Marko and E. D. Siggia, Stretching DNA, *Macromolecules* **28**:8759–8770 (1995).
30. C. Bouchiat, M. D. Wang, J.-F. Allemand, T. R. Strick, S. M. Block, and V. Croquette, Estimating the persistence length of a Worm-Like Chain molecule from force-extension measurements, submitted to *Biophys. J.* (1998).
31. M. D. Wang, H. Yin, R. Landick, J. Gelles, and S. M. Block, Stretching DNA with optical tweezers, *Biophys. J.* **72**:1335–1346 (1997).
32. C. Baumann, S. Smith, V. Bloomfield, and C. Bustamante, Ionic effects on the elasticity of single DNA molecules, *Proc. Natl. Acad. Sci. (USA)* **94**:6185–6190 (1997).
33. S. B. Smith, Y. Cui, and C. Bustamante, Overstretching B-DNA: The elastic response of individual double-stranded and single-stranded DNA molecules, *Science* **271**:795–799 (1996).
34. A. Lebrun and R. Lavery, Unusual DNA conformations, *Curr. Op. Struct. Biol.* **7**:348–354 (1997).
35. J. Marko, DNA under high tension: Overstretching, undertwisting and relaxation dynamics, *Phys. Rev. E* **57**:2134–2149 (1998).
36. J. Sambrook, E. F. Fritsch, and T. Maniatis, *Molecular Cloning: A Laboratory Handbook* (Cold Spring Harbor Laboratory Press, 1989).
37. J. D. Watson, M. Gilman, J. Witkowski, and M. Zoller, *Recombinant DNA* (Scientific American Books, Inc., 1992).
38. B. Essevaz-Roulet, U. Bockelmann, and F. Heslot, Mechanical separation of the complementary strands of DNA, *Proc. Natl. Acad. Sci. (USA)* **94**:11935–11940 (1997).
39. T. R. Strick, J.-F. Allemand, D. Bensimon, and V. Croquette, Behavior of supercoiled DNA, *Biophys. J.* **74**:2016–2028 (1998).
40. E. Palecek, Local supercoil-stabilized structures, *Crit. Rev. Biochem. Mol. Biol.* **26**:151–226 (1991).
41. D. Kowalski, D. Natale, and M. Eddy, Stable DNA unwinding, not breathing, accounts for single-strand-specific nuclease hypersensitivity of specific A + T-rich sequences, *Proc. Natl. Acad. Sci. (USA)* **85**:9464–9468 (1988).
42. C. J. Benham, Energetics of the strand separation transition in superhelical DNA, *J. Mol. Biol.* **225**:835–847 (1992).
43. T. C. Boles, J. H. White, and N. R. Cozzarelli, Structure of plectonemically supercoiled DNA, *J. Mol. Biol.* **213**:931–951 (1990).
44. J. F. Marko and E. D. Siggia, Fluctuations and supercoiling of DNA, *Science* **265**:506–508 (1994).
45. J. F. Marko and E. D. Siggia, Statistical mechanics of supercoiled DNA, *Phys. Rev. E* **52**:2912–2938 (1995).
46. J. F. Marko, Supercoiled and braided DNA under tension, *Phys. Rev. E* **55**:1758–1772 (1997).

47. C. Bouchiat and M. Mézard, Elasticity model of a supercoiled DNA molecule, *Phys. Rev. Lett.* **80**:1556–1559 (1998).
48. J. D. Moroz and P. Nelson, Torsional directed walks, entropic elasticity and DNA twist stiffness, *Proc. Natl. Acad. Sci. (USA)* **94**:14418–14422 (1998).
49. D. Bensimon, Force: A new structural control parameter? *Structure* **4**:885–889 (1996).
50. H. Noji, R. Yasuda, M. Yoshida, and K. Kinosita, Jr., Direct observation of the rotation of F1-ATPase, *Nature* **386**:299–302 (1997).
51. A. Ishijima, H. Kojima, T. Funatsu, M. Tokunaga, H. Higuchi, H. Tanaka, and T. Yanagida, Simultaneous observation of individual ATPase and mechanical events by a single myosin molecule during interaction with actin, *Cell* **92**:161–171 (1998).
52. K. Svoboda, C. F. Schmidt, B. J. Schnapp, and S. M. Block, Direct observation of kinesin stepping by optical trapping interferometry, *Nature* **365**:721–727 (1993).